

Periodogram and likelihood periodicity search in the SNO solar neutrino data

Gioacchino Ranucci and Marco Rovere

Istituto Nazionale di Fisica Nucleare

Via Celoria 16, 20133 Milano, Italy

e-mail: gioacchino.ranucci@mi.infn.it, marco.rovere@mi.infn.it

ABSTRACT

In this work a detailed spectral analysis for periodicity search of the time series of the ^8B solar neutrino flux released by the SNO Collaboration is presented. The data have been publicly released with truncation of the event times to the unit of day (1 day binning); they are thus suited to undergo the traditional Lomb-Scargle analysis for periodicity investigation, as well as an extension of such a method based on a likelihood approach. The results of the analysis presented here confirm the absence of modulation signatures in the SNO data. For completeness, it is also illustrated a more refined “1 day binned” likelihood, which approximates the unbinned likelihood methodology, based upon the availability of the full time information, adopted by the SNO collaboration.

Key words: time series analysis, solar neutrinos, likelihood, periodogram

PACS: 95.75.Wx, 26.65.+t, 07.05.Kf

1. Introduction

Recently the SNO collaboration published the results of the periodicity search performed on the measured time series of the ^8B neutrino flux [1], and afterwards released publicly the raw data used in the analysis [2]. In this work we present the results obtained performing alternative periodicities investigations on the released datasets. The basic tool adopted for this investigation is the estimation of the frequency spectrum of the neutrino flux times series, since it is well known that periodicities hidden in the data would appear as sharp peaks in the spectrum itself. The important and crucial part of the analysis, however, is not the calculation of the spectrum, but the precise assessment of the statistical significance of the most prominent experimental spectral peaks, since the noise affecting the data series produces erratic peaks which can attain also very high values.

Hence a large part of the paper is devoted to such significance evaluation, performed following a Monte Carlo procedure well established in [3] and [9]. Such an analysis is complemented by the determination of the sensitivity of the method for the discovery of a true oscillation embedded in the data, which will obviously depend upon the amplitude and frequency of the hypothetical signal.

The paper is organized as follows: in paragraph 2 a brief description of the data is given (essentially a short summary of the thorough description reported in [1]), in paragraph 3 there is the illustration of the two different data analysis procedures adopted, paragraph 4 is devoted to the significance assessment of the largest detected peaks via the Monte Carlo determination of the null hypothesis distributions, in paragraph 5 the sensitivity of the methods for the discovery of true modulations is reported, in paragraph 6 the features of the analysis results at two specific frequencies of interest are described, in paragraph 7 it is illustrated a procedure which approximates the features of an unbinned likelihood analysis, and finally in paragraph 8 there are the conclusions.

2. Description of the data sets

It is well known that the SNO detector is an heavy water Cerenkov detector which measures ^8B solar neutrinos via charged-current and neutral-current interactions on deuterons in 1 kton of D_2O , and also through neutrino-electron elastic scattering interactions.

The datasets used in this analysis, officially released by the SNO collaboration, are similar to those used in the periodicity search reported in [1]. They are related to the two first phases of the experiment, i.e. the pure D_2O phase and the salt phase, when salt has been added to the heavy water in order to increase the neutron detection efficiency. The data taking period started on November 2, 1999 and encompassed in total about 1400 calendar days.

Specifically the SNO collaboration released for both phases two files, one with the number of daily detected events, and the other with the specification of the runtime periods during each day of data taking. A proper periodicity analysis clearly has to take into account the actual live time within each day of data taking in order to properly normalize the detected counts. It must be pointed out that there is a difference between the released data and those used by the SNO Collaboration in its periodicity search: while the latter retain the full time information, the former are characterized by the rounding of the time of each event to the units of day. Practically this implies that the data have been published in the format of 1 day binning.

The event rates vs. time, obtained trough a suitable bin manipulation similar to that used in [1], are displayed in Fig. 1 and 2 for the D_2O and salt phase, respectively. In particular, some of the nominal 1 day bins have been merged together when the respective width was much shorter than the nominal value, in order to avoid large scattering in the data display. The rate is 9.35 ev/day in the case of the D_2O phase, and 11.85 ev/day in the case of the salt phase. The fact the shape of the two figures reproduces well also the details of the two corresponding figures in [1] gives confidence that the retrieval and arrangement of the data have been done properly.

In particular, each point of the series in the two figures is characterized by a time value which is the weighted mean time of the corresponding bin, evaluated so to take into account

properly the bin live time, and by a corresponding ordinate value which is the normalized count rate in the same bin, i.e. the total counts in that bin divided by the corresponding live time.

This summary description of the data is enough for the purpose of the present analysis. For further details on the characteristics of the datasets the reader can refer to [1].

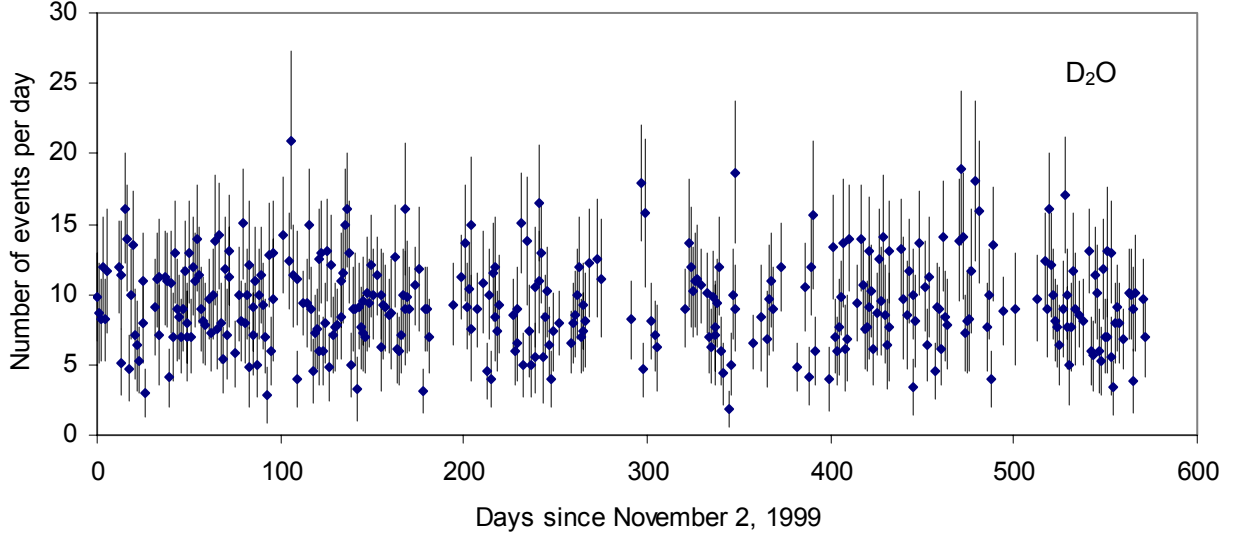


Fig. 1 – D₂O phase event rate

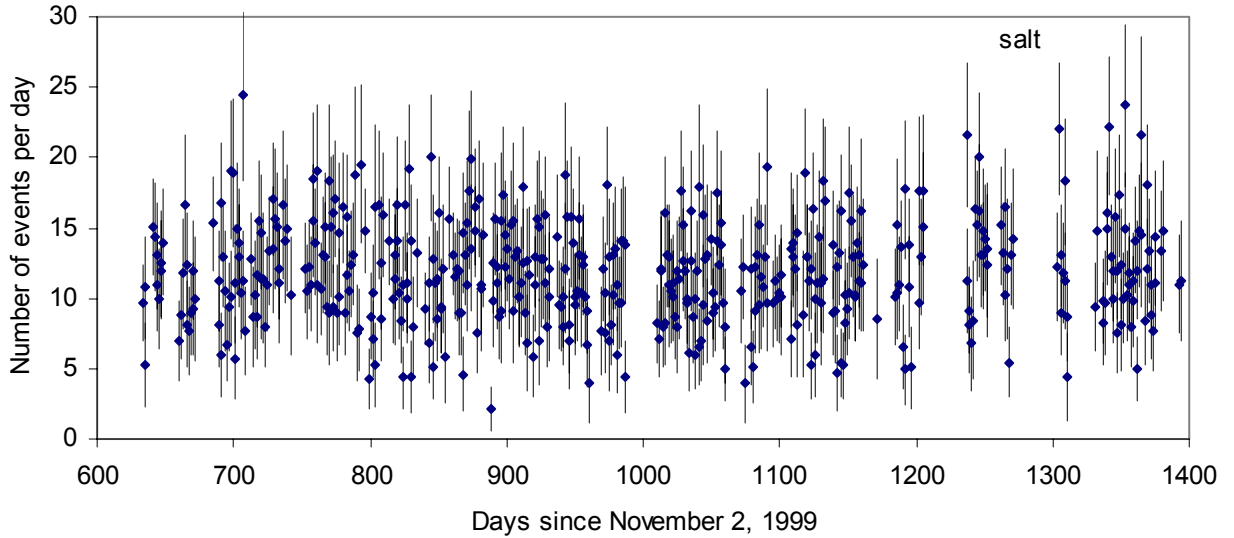


Fig. 2 – Salt phase event rate

3. Spectral data analysis methods and spectra

In the periodicity search published by SNO the main tool of analysis is an unbinned maximum likelihood scan of the data, which exploits fully the time information for each neutrino event. Because of the rounding in the released data of the neutrino event times to the unit of day mentioned above, the same exact analysis methodology cannot be applied here. Furthermore, in [1] a second analysis has been presented based on the so called weighted Lomb-Scargle method [4].

Instead, for the present analysis two alternative approaches have been chosen, which somehow complement those adopted by the SNO collaboration: a) the standard (not weighted) Lomb-Scargle periodogram search and b) a likelihood extension of the Lomb-Scargle search itself.

3.1 Lomb Scargle method

3.1.1 Statistical properties

Traditionally the Lomb-Scargle spectrum (denoted more frequently as periodogram) is the standard tool for the spectral analysis of time series composed by unevenly spaced points.

The data as displayed in Fig. 1 and 2 are already arranged in a suitable way to undergo such a standard methodology; indeed, the data in this format reproduce an unevenly sampled time series, thanks to the arrangement to represent an extended bin via a single weighted mean live time (it may be worth to remind that the same format was used in the data released by the Super-Kamiokande collaboration [5]). On the other hand, the ordinate values may be considered as sampled by a continuous function representing the count rate vs. time.

By denoting with t_r the sequence of time values, with x_r the corresponding measured values and with F the average value of the whole series, the Lomb-Scargle periodogram is computed as [6] [7] [9].

$$\frac{1}{2\sigma^2} \left(\frac{\left(\sum_{r=1}^N (x_r - F) \cos \omega(t_r - \tau) \right)^2}{\sum_{r=1}^N \cos^2 \omega(t_r - \tau)} + \frac{\left(\sum_{r=1}^N (x_r - F) \sin \omega(t_r - \tau) \right)^2}{\sum_{r=1}^N \sin^2 \omega(t_r - \tau)} \right) \quad (1)$$

where

$$\frac{\sum_{r=1}^N \sin 2\omega t_r}{\sum_{r=1}^N \cos 2\omega t_r} = \tan 2\omega \tau \quad (2)$$

and

$$\sigma^2 = \frac{1}{N-1} \sum_{r=1}^N (x_r - F)^2 \quad (3).$$

The Lomb-Scargle periodogram is characterized by well defined statistical properties described for example in [7] and recently reviewed in [8]. Here the main aspects of such properties are reminded. In case of the null hypothesis that the series is sampled by a pure Gaussian noise process with no modulation embedded, the periodogram ordinate at each frequency follows a simple exponential distribution e^{-z} ; such an exponential distribution is the basis of the false alarm probability formula introduced in [7] and [9] to perform the significance assessment of the largest detected peak in the periodogram. This false alarm formula, which is

$$P(> z) = 1 - (1 - e^{-z})^M \quad (4)$$

where M is the number of independent scanned frequencies in the search for periodicities, stems from the probability density function of the height of the largest spectral peak in case of pure noise series: if the frequencies are M , each individually exponentially distributed, the PDF of the largest value is obviously

$$p_{largest}(h) = M \left[1 - e^{-h} \right]^{M-1} e^{-h} \quad (5)$$

from which the integration above a threshold z gives the (4).

Hence in practice, the quantification of the consistency (or inconsistency) of a time series with the hypothesis of constant rate according to the Lomb-Scargle method requires simply to compute its spectrum, to note the maximum spectral peak z_{max} and to evaluate, by substituting z_{max} in the (4), the probability to get an ordinate as high or higher than z_{max} by pure noise chance: as a consequence the statistical significance of the peak is high (i.e. likely it is actually due to a true signal) if the false alarm formula gives a low or very low value.

This methodology is not ambiguous if M is known. However M is exactly known only in the particular case of even sampling [9]. In the practical cases of uneven sampling M is not easily a-priori defined: it depends on the coherence of the series and it is heuristically interpreted as the effective number of independent scanned frequencies; in such a situation the above simple analytical procedure is more effectively replaced by a Monte Carlo approach (see for example [3] and [9]): many modulation free synthetic time series with the same timing and statistical (in this case of Poisson nature) properties of the experimental series under study are generated, for each of them the relevant spectrum is computed, and the maximum values of all the spectra are used to create the histogram which represent the so called null hypothesis distribution, i.e. the maximum spectral peak distribution under the assumption of pure noisy series. The significance of the largest spectral peak z_{max} in the actual spectrum of the experimental series is then obtained reading off the Monte Carlo histogram the fraction of times in which the simulation produced a value as high or higher than z_{max} itself.

The Monte Carlo output can also be used to determine the number M of effectively scanned frequencies, being for this purpose simply required to evaluate the value of M which ensures the best fit of the simulated null hypothesis distribution to the relation (5).

The standard approach described above considers only the highest spectral peak as diagnostic element to judge the consistency (or inconsistency) of the series with the constant rate assumption. More insight on the feature of the series, however, can be obtained by extending such a statistical treatment also to the other spectral peaks (practically, to the bunch of the more prominent peaks). In particular, by ordering the peaks at the various frequencies over the search band in term of their height, it is possible to generalize the (5) in order to express analytically the distribution of the height of the lowest peak, of the second lowest peak and so on, up to the highest peak, in case of pure white noise time series. How to perform such generalization (in the different context of photoelectron statistics) has been shown in [10] and [11]: still denoting the number of independent frequencies with M , the probability density function of the spectrum ordinate of the i_{th} (in term of height, starting from the lowest) spectral peak is

$$p_i(h/M) = \frac{M!}{(i-1)!(M-i)!} [1 - F(h)]^{(M-i)} [F(h)]^{i-1} p(h) \quad (6)$$

where

$$F(h) = \int_0^h p(\lambda) d\lambda \quad (7)$$

being $p(h)$ simply e^{-h} .

As cross check it can be easily verified that the (6) reduces to the (5) in case of the highest peak.

The Monte Carlo extension of the procedure is quite straightforward, since it requires only to evaluate, in addition to the null hypothesis distribution of the highest peak, those of the second highest, third highest and so on peaks (in the present analysis such an extension has been limited to the first four highest peaks). The model functions (6) in the following will be used to model the curves obtained from the Monte Carlo calculations.

It should be noted that, strictly speaking, the statistical properties of the Lomb-Scargle periodogram summarized in this section are valid in the assumption of time series affected by Gaussian noise; instead, the count process generating the time series of the measured SNO data is obviously of Poisson nature. The comparison of the model with the Monte Carlo in paragraph 4 will show, however, that the above results maintain their validity also in this case.

3.1.2 Experimental spectra

Due to the 1 day binning of the released data, the corresponding frequency analysis is characterized by a Nyquist frequency which is about 0.5 cycle/days (or in term of years about 180 cycles/years). The spectra presented in this section (as well as those of section 3.2.2) are thus limited up to such frequency boundary (note: the ordinate of the periodogram is denoted as Power).

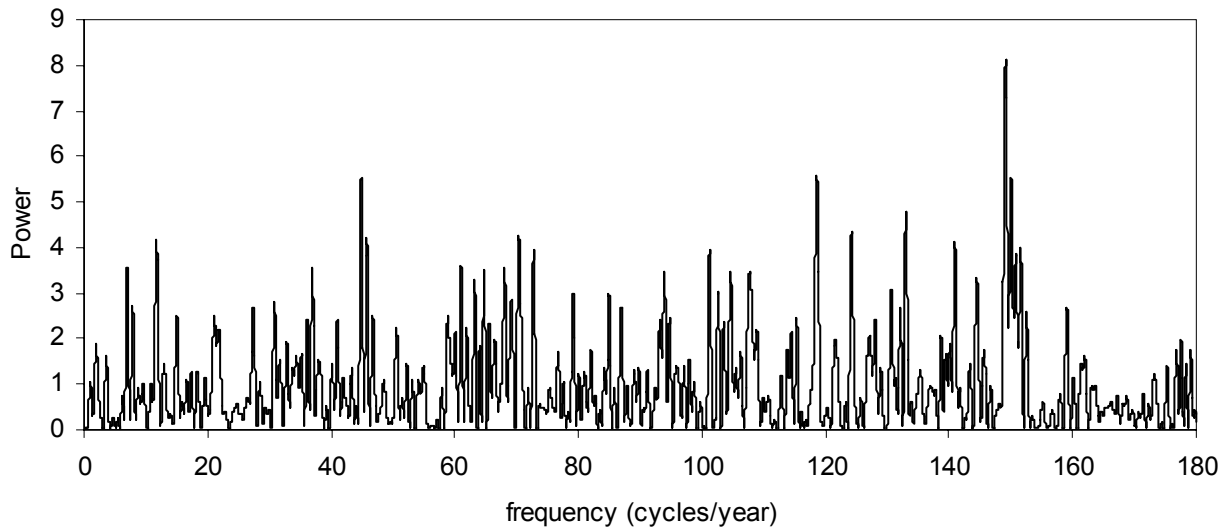


Fig. 3 – D_2O phase Lomb-Scargle periodogram

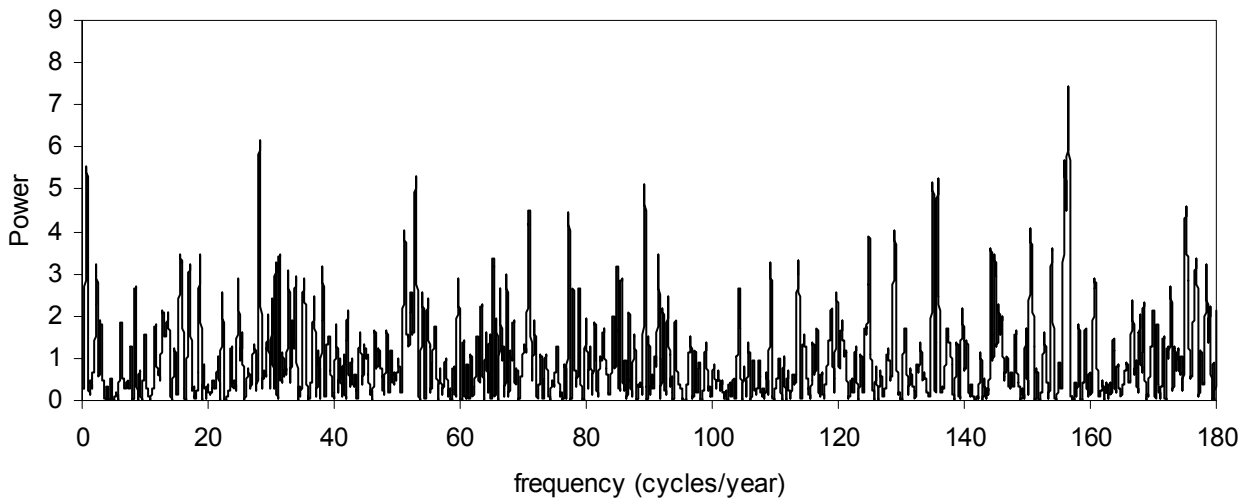


Fig.4 – Salt phase Lomb-Scargle periodogram

The three periodograms related to the D₂O phase, the salt phase and the combined dataset obtained via application of the (1), (2) and (3) are shown in Fig. 3, 4 and 5 (the analysis of the combined dataset has been performed after scaling the values of the salt period in order to equalize the average count rate of both phases).

In the spectrum in Fig. 3 the four highest peaks have, respectively, ordinates 8.11 (149.13), 5.59 (118.6), 5.55 (44.86) and 5.54 (150.03) (in the brackets there are the corresponding frequencies expressed in cycles/year).

In the spectrum in Fig. 4 the major peaks are, respectively, 7.43 (156.52), 6.16 (28.15), 5.55 (0.75) and 5.32 (52.93).

Finally, in the combined spectrum in Fig. 5 the major peaks are 7.54 (150.66), 6.13 (36.84), 5.99 (70.76) and 5.87 (118.56).

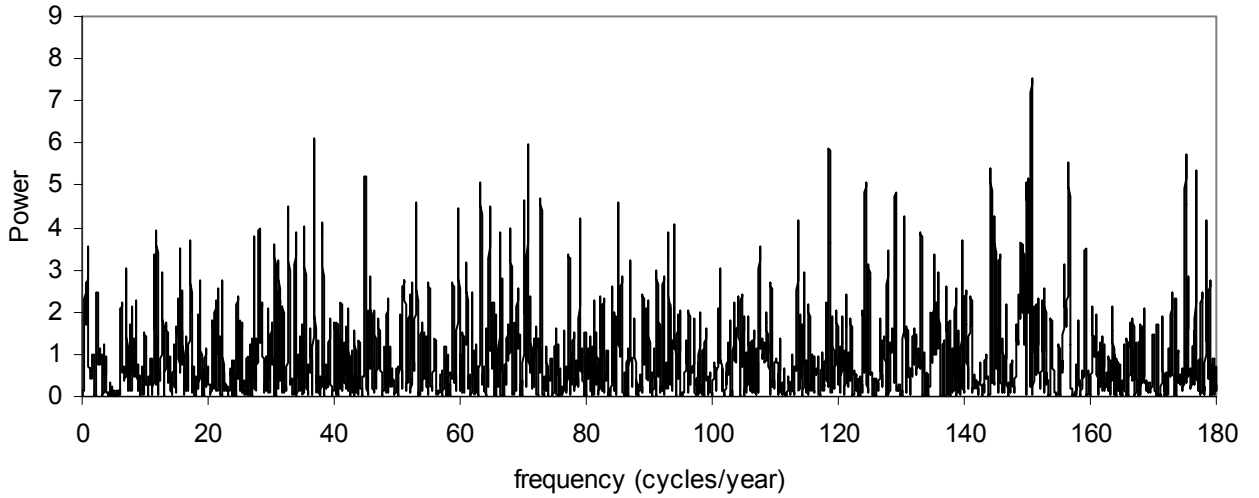


Fig.5 – Combined dataset Lomb-Scargle periodogram

The discussion of the consistency of these spectra with the hypothesis of constant rate will be addressed in the next paragraph 4, where the issue of the significance of the major peaks identified in each of them will be performed following the Monte Carlo procedure described before.

3.2 Likelihood generalization of the Lomb-Scargle method

3.2.1 Methodology and statistical properties

In various works (for example [12], [8]) it has been explained how the standard Lomb-Scargle search can be generalized via a likelihood method that allows to take into account fully the probabilistic nature of the underlying process generating the series under study, i.e. in the present case the Poisson nature of the counting process.

For the problem being considered such an extension can be performed as follows; by denoting the variable average neutrino flux as

$$\mu(t) = \mu_{\cos t} [1 + a \cdot \sin(\omega t + \varphi)] \quad (8)$$

we have that the expected mean rate for the r_{th} bin, represented by the weighted mean time t_r , can be written as

$$\mu_r = \mu(t_r) \Delta t_r \quad (9)$$

where Δt_r is the width of the bin itself; the likelihood for the detected sequence of values is consequently

$$L = \prod_{r=1}^N \frac{\mu_r^{n_r} e^{-\mu_r}}{n_r!} \quad (10)$$

n_r being the number of counts in the r_{th} bin. μ_{cost} is the average count rate evaluated separately for the D₂O and salt phases, and a and φ are the amplitude and phase maximization parameters.

Resorting to the Wilks' theorem (or log-likelihood ratio theorem) [13] the generalized likelihood ratio can be written as

$$GLR = \frac{\prod_{r=1}^N \frac{\mu_{cost}^{n_r} e^{-\mu_{cost}}}{n_r!}}{\max_{a,\varphi} \prod_{r=1}^N \frac{\mu_r^{n_r} e^{-\mu_r}}{n_r!}} \quad (11)$$

with the theorem stating that the quantity $-\ln(GLR)$

$$-\ln(GLR) = S(\omega) = \max_{a,\varphi} \sum_{r=1}^N (-\mu_r + n_r \cdot \ln \mu_r) - \sum_{r=1}^N (-\mu_{cost} + n_r \cdot \ln \mu_{cost}) \quad (12)$$

is exponentially distributed as e^{-S} under the null hypothesis; $S = -\ln(GLR)$ is by definition the likelihood spectrum of the process. The likelihood spectrum thus shares the same property of the Lomb-Scargle periodogram that the spectral ordinate at each frequency in case of pure noise follows an exponential distribution. As a consequence, it can be presumed that the distribution of the highest peak follows the (5) and that more in general the distributions of the peaks ranked in term of height should follow the (6).

Clearly, also in the framework of the likelihood method a Monte Carlo approach similar to that outlined for the Lomb-Scargle case can be adopted to assess the significance of the largest peaks. In the relevant studies reported in paragraph 4 it will be checked how faithfully the formulas (5) and (6) are able to reproduce the actual Monte Carlo histograms.

3.2.2 Experimental spectra

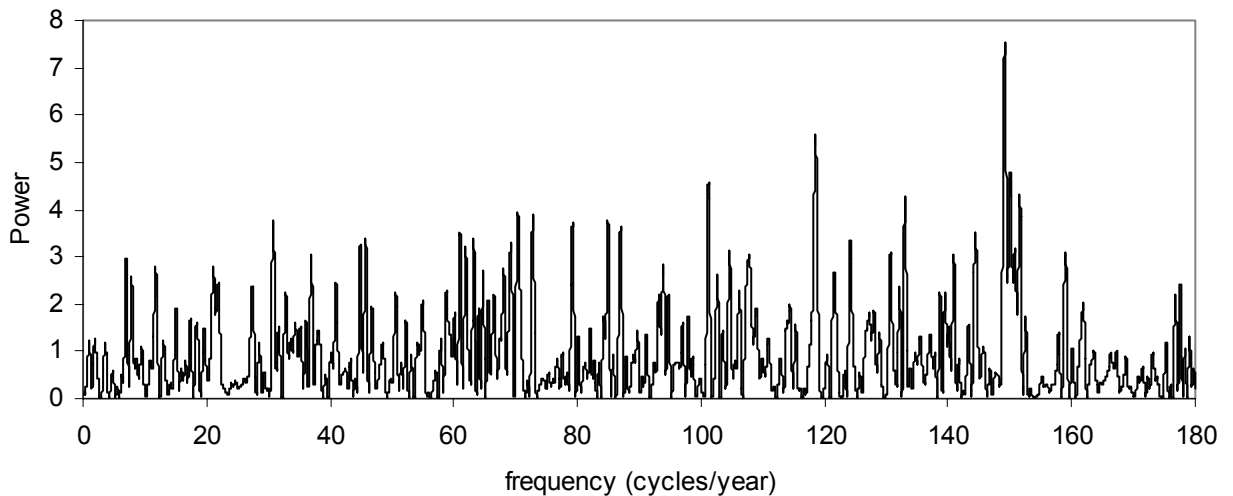


Fig.6 – D₂O phase likelihood spectrum

The spectra computed according to the (12) for the D₂O phase, the salt phase and the combined dataset are shown in Fig. 6, 7 and 8.

In the spectrum in Fig. 6 the four highest peaks have, respectively, ordinates 7.53 (149.16), 5.58 (118.53), 4.8 (150.08) and 4.55 (101.19) (again in parenthesis there are the corresponding frequencies in cycles/year).

In the spectrum in Fig. 7 the four highest peaks have, respectively, ordinates 6.18 (156.53), 6.01 (52.91), 5.46 (28.16) and 5.04 (0.75).

Finally, in the spectrum in Fig. 8 related to the combined dataset the four highest peaks have ordinates 6.84 (150.67), 5.85 (36.84), 5.41 (144.24) and 5.31 (53.03).

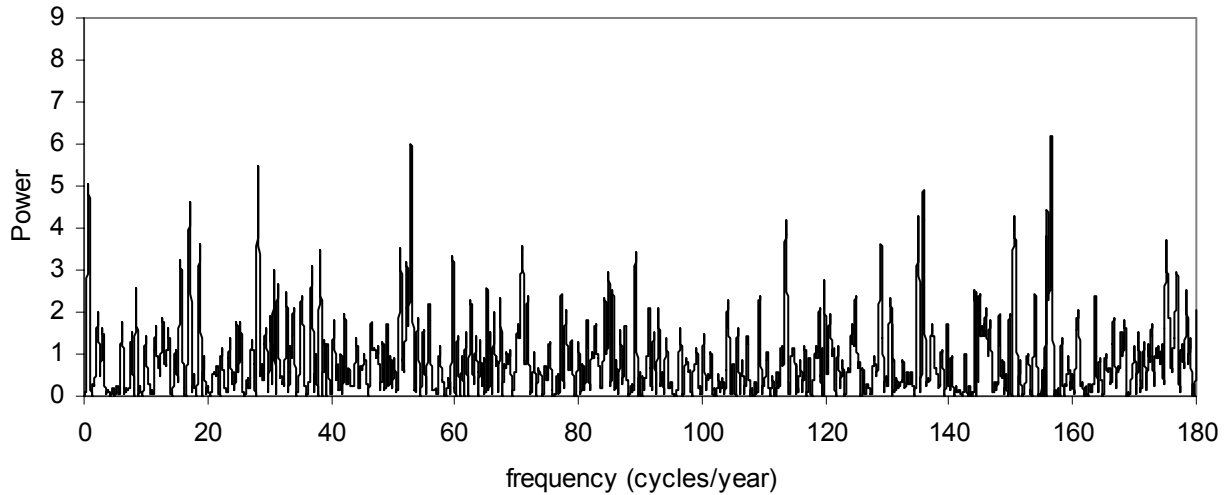


Fig.7 – Salt phase likelihood spectrum

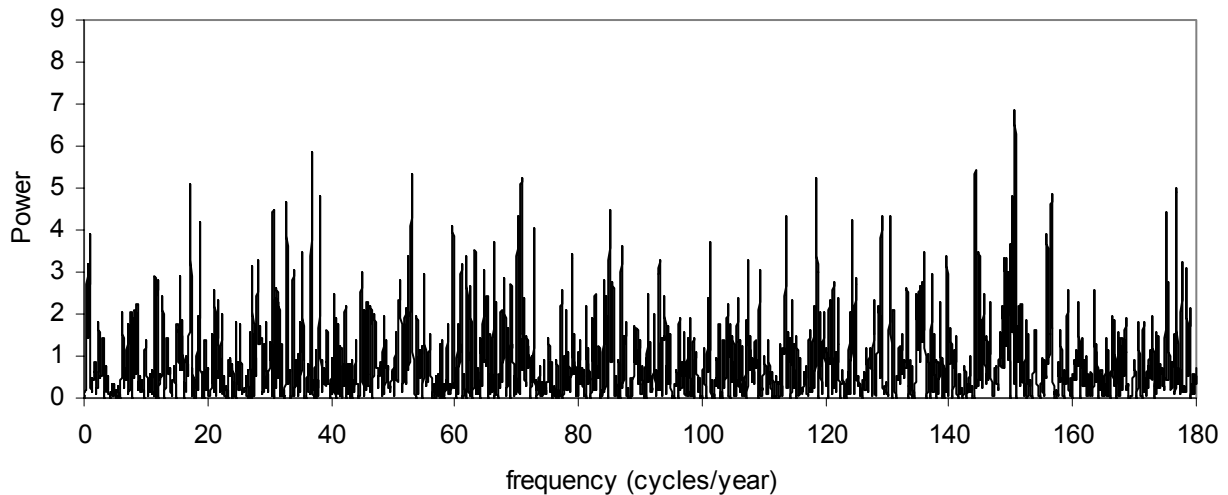


Fig.8 – Combined dataset likelihood spectrum

We move now to the Monte Carlo significance assessment via the extensive Monte Carlo studies reported in the next paragraph

4. Null hypothesis distributions and significance assessment

All the reference null hypothesis Monte Carlo distributions reported in this paragraph, computed as extensively explained in paragraph 3, have been inferred from 10000 simulation cycles; in each cycle a synthetic series is generated and the relevant spectrum is computed.

Specifically, each ordinate value of the synthetic series is generated by drawing a random number from a Poisson distribution with mean value equal to the product of the experimental average rate times the live time of the corresponding bin, and then by dividing the drawn number by the live time itself. In this way the simulated series automatically retain timing and statistical properties of the experimental series.

In the following, after describing the features of the simulated distributions, the significances of the major spectral peaks are listed both for the Lomb-Scargle and likelihood method. As consistency check, it must be added that we verified throughout the simulation process how precisely the individual frequencies of the simulated spectra follow the predicted exponential distribution, finding a perfect agreement between the simulation results and the theoretical expectations for both methodologies.

4.1 Lomb-Scargle distributions

The Lomb Scargle null hypothesis distributions for the D₂O phase, salt phase and the combined dataset are reported in Fig. 9, 10 and 11, respectively. In each figure there are the distributions of the four highest peaks, as well as the plots of the model functions (6).

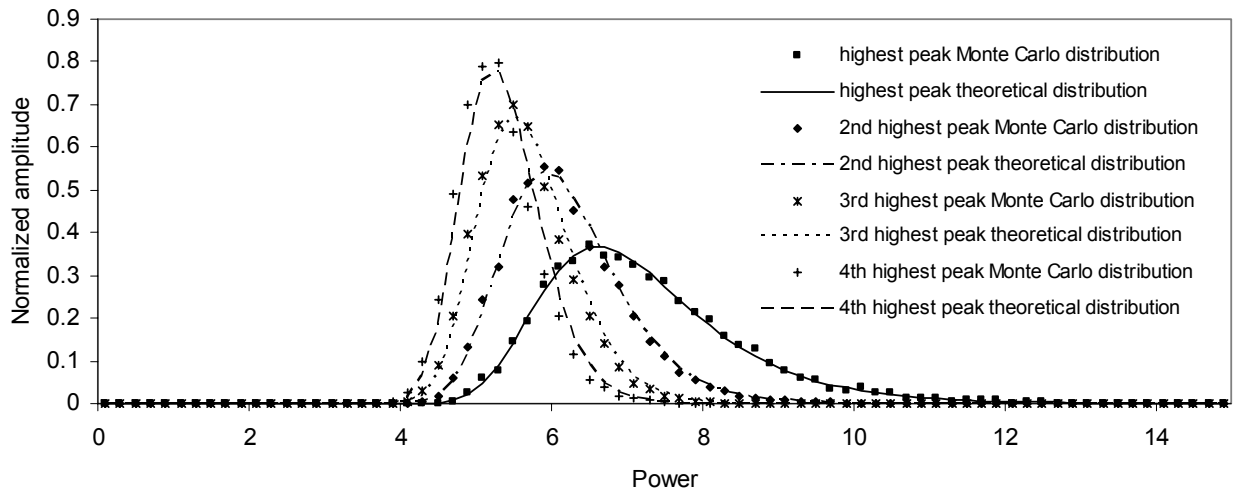


Fig. 9 – D₂O phase null hypothesis distributions (Lomb-Scargle method)

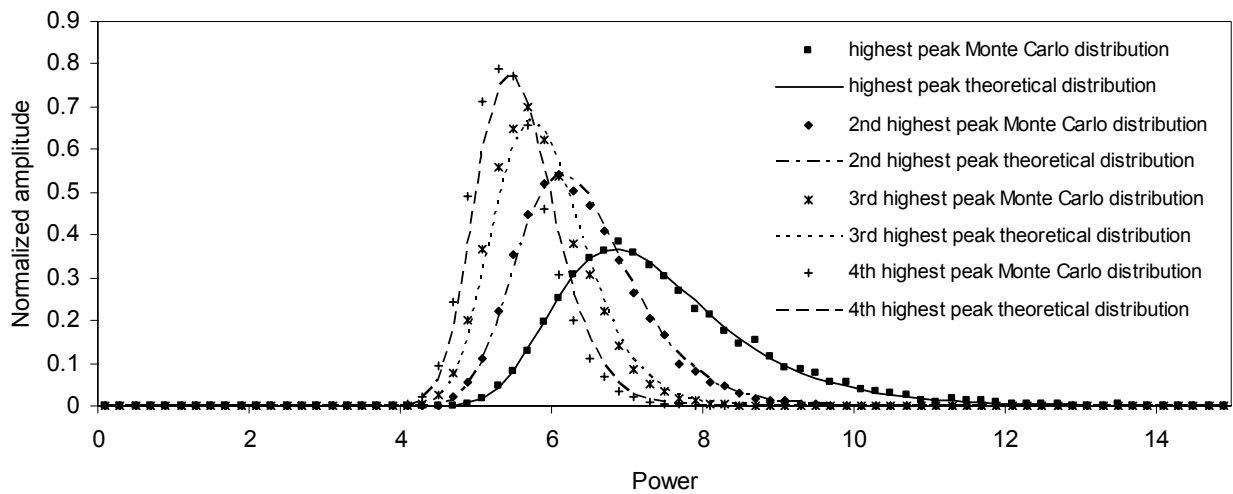


Fig. 10 – Salt phase null hypothesis distributions (Lomb-Scargle method)

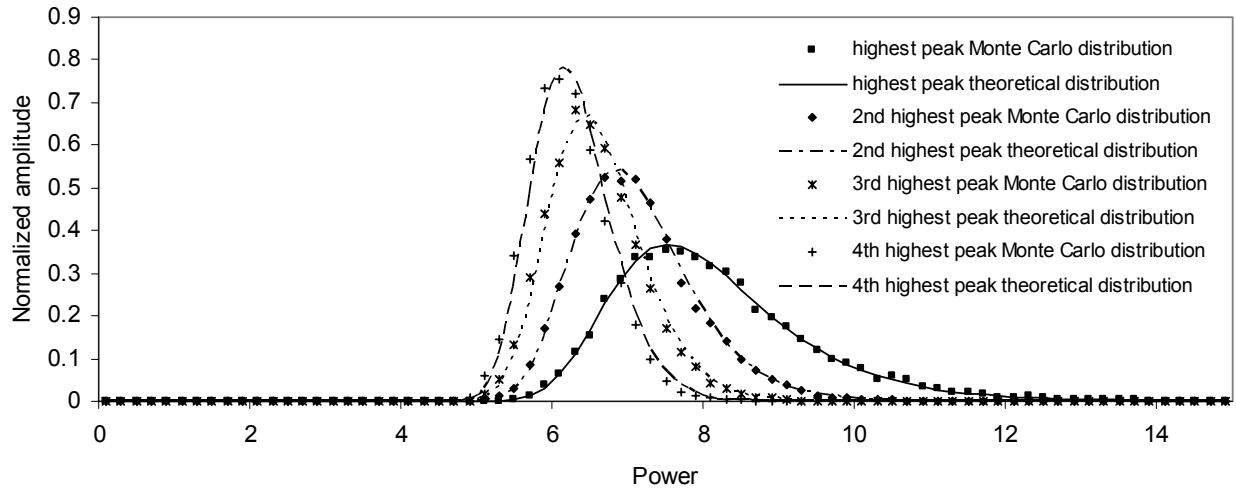


Fig. 11 – *Combined dataset null hypothesis distributions (Lomb-Scargle method)*

It is worth to point out that the model functions are normalized to unit area, and thus for comparison purpose also the Monte Carlo curves have been normalized in the same way.

It can be noted that the Monte Carlo distributions of the peaks (the analysis is limited to the four highest peaks) follow remarkably well the model functions with a number of effective independent frequencies equal to 752 for the D₂O dataset, 936 for the salt dataset and 1876 for the combined dataset. Such numbers have been obtained through the fit to the model (5) of the distribution pertaining to the highest spectral peak. A slight disagreement, however, can be noted for the curves related to the third and fourth peaks. Even though it can be shown [8] that the perfect agreement of the simulated curves to the general model (6) is expected only in the case of evenly sampled time series, when the Lomb-Scargle periodogram reduces to the so called Schuster periodogram [7], the good agreement of the model to the Monte Carlo distributions in the Lomb-Scargle case is not a surprise, since it was already demonstrated via extensive simulations in [3], at least for the highest peak.

As illustrated before, from the simulated distributions we can get the significance of the four highest peaks of each spectrum; the results are summarized in the tables 1, 2 and 3, respectively. In no cases there are “interesting” low or very low significance levels, and hence the values in the tables taken all together show unambiguously that the three spectra are very well consistent with the hypothesis that the SNO data time series are due to a constant rate process.

Ordinate	Frequency	Significance
8.11	149.13	20.7%
5.59	118.60	75.5%
5.55	44.86	51.7%
5.54	150.03	27.7%

Table 1 -. D₂O Lomb-Scargle significance.

Ordinate	Frequency	Significance
7.43	156.52	42.9%
6.16	28.15	56.4%
5.55	0.75	65.9%
5.32	52.93	58.9%

Table 2 -. Salt Lomb-Scargle significance.

Ordinate	Frequency	Significance
7.54	150.66	63.4%
6.13	36.84	90.7%
5.99	70.76	82.1%
5.87	118.56	72.2%

Table 3 -. Combined data set Lomb-Scargle significance.

4.2 Distributions for the likelihood generalization of the Lomb-Scargle method

The null hypothesis distributions for the D₂O phase, salt phase and the combined dataset stemming from the application of the likelihood generalization of the Lomb-Scargle method are reported in Fig. 12, 13 and 14. Also in these figures there are the distributions of the four highest peaks overlapped to the respective model functions (6).

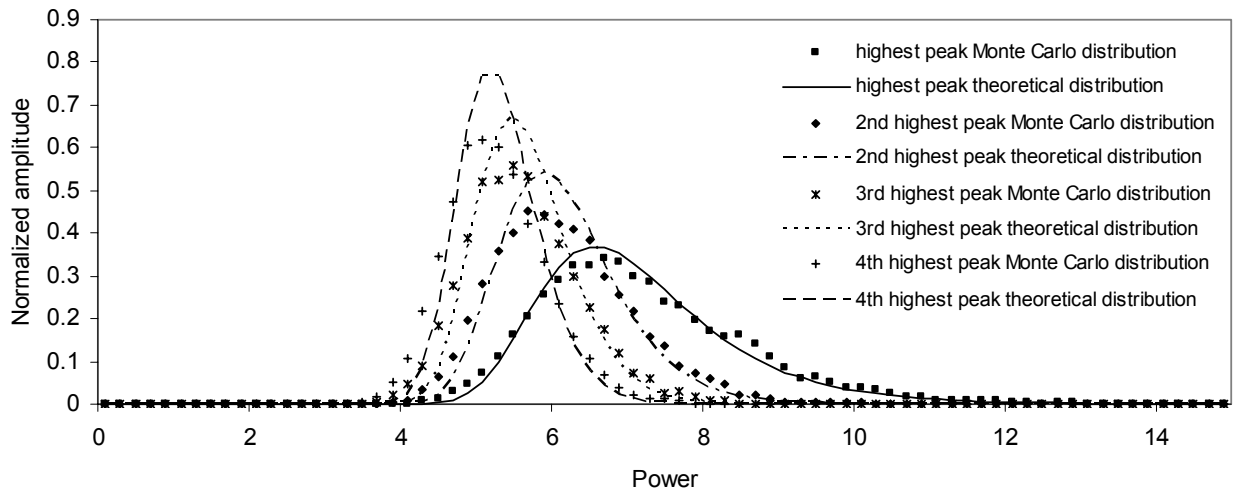


Fig. 12 – D₂O phase null hypothesis distributions (likelihood method)

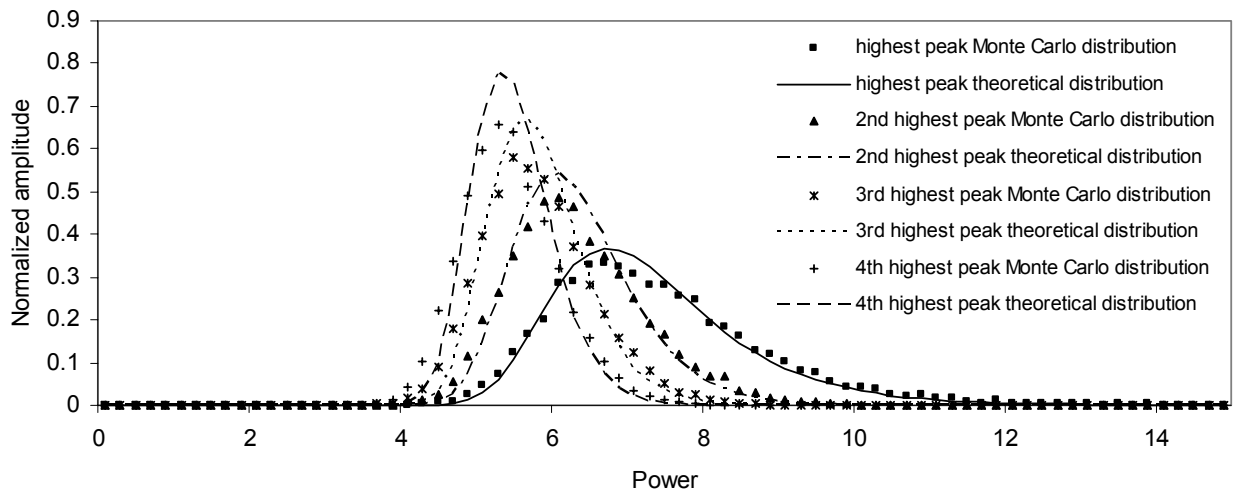


Fig. 13 – Salt phase null hypothesis distributions (likelihood method)

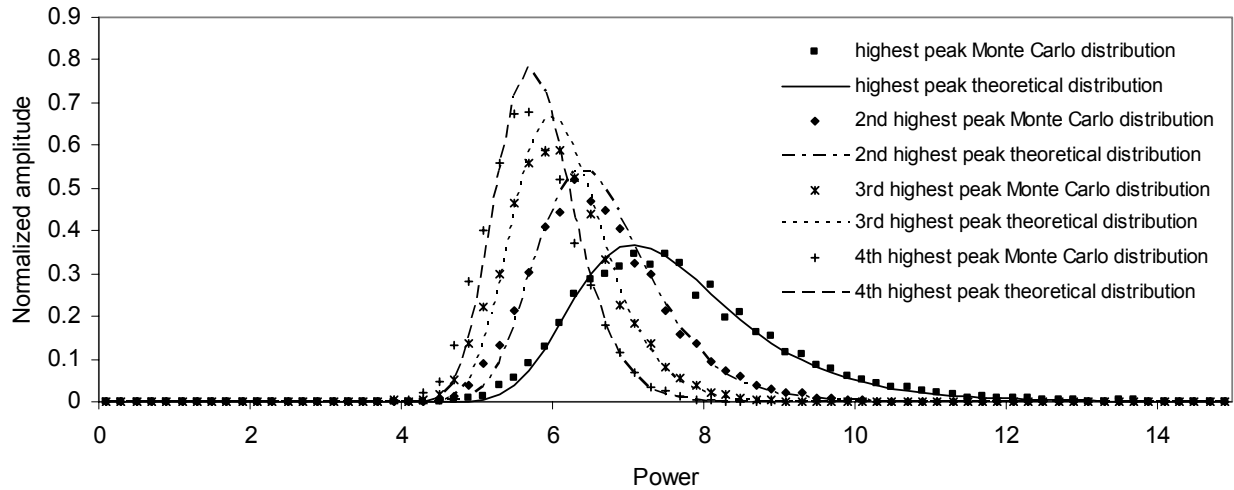


Fig. 14 – Combined dataset null hypothesis distributions (likelihood method)

Ordinate	Frequency	Significance
7.54	149.16	34.5%
5.58	118.53	71.5%
4.80	150.08	87.5%
4.55	101.19	86.9%

Table 4 -. D2O Likelihood significance.

Ordinate	Frequency	Significance
6.18	156.53	81.7%
6.02	52.91	60.6%
5.46	28.16	66.1%
5.04	0.75	73.4%

Table 5 -. Salt Likelihood significance.

Ordinate	Frequency	Significance
6.84	150.67	71.7%
5.85	36.84	82.2%
5.41	144.24	84.8%
5.31	53.03	76.3%

Table 6 -. Combined Likelihood significance

It can be noted that now the peak distributions follow only approximately the model functions, far from the good agreement observed in the Lomb-Scargle case. Specifically, the value M obtained through the approximate fit of the highest peak distribution to the equation (5) equals 724, 856 and 1196 in the D2O, salt and combined datasets, respectively. The significance of the four major peaks in each spectrum, inferred from the corresponding null hypothesis distributions, are summarized in the tables 4, 5 and 6. By examining the values in the tables it can be immediately concluded that also this alternative methodology demonstrates that all the three spectra are fully consistent with the hypothesis of a constant rate time series.

5. Sensitivity of the methods to true periodicities

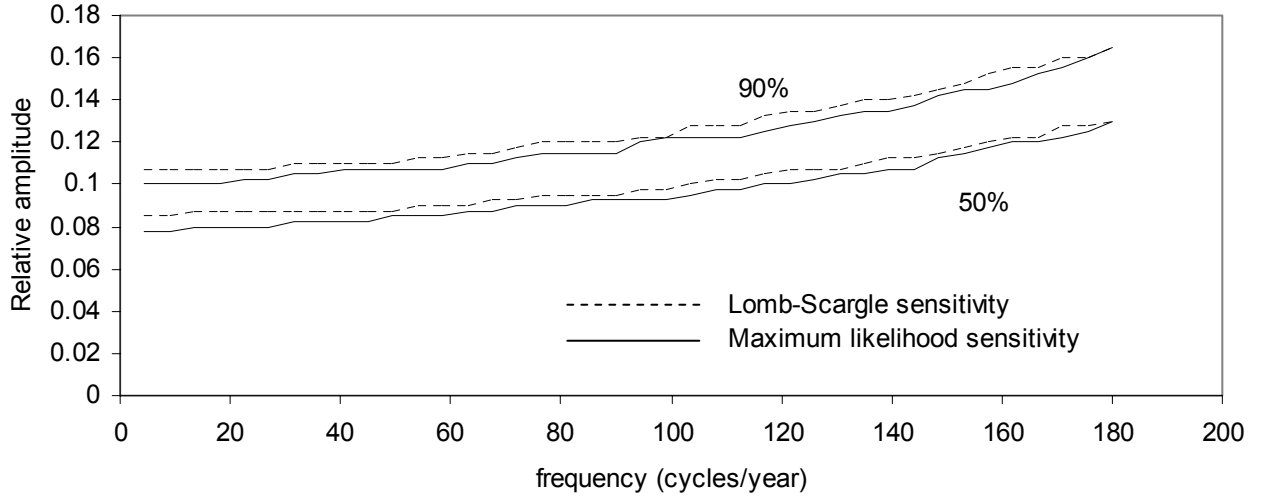


Figure 15 – Sensitivity contours

The sensitivity of the two methods under consideration to a true periodicity can be evaluated by defining a desired confidence level for a discovery claim, for example 99%, which is equivalent to fix a detection threshold on the null hypothesis distribution producing a false detection only in 1% of the cases; then via Monte Carlo it is determined for each frequency the modulation amplitude that, above the selected threshold, ensures a detection at a prescribed level of probability, for example 50% and 90%. The noise distribution to consider to set the detection threshold is clearly that relevant to the highest spectral peak.

The 50% and 90% sensitivity contours for the confidence level of 99% are shown in Fig. 15 for both the Lomb-Scargle and likelihood methods. It can be noted that the sensitivities of the two approaches are pretty similar, the likelihood method being only marginally better than the Lomb-Scargle one.

Such curves can be compared with those reported in [1]. In particular, apart from the different scale on the x axis, the contours for the Lomb-Scargle method computed here appear to be close to those for the weighted Lomb-Scargle method reported in the figure 4 of [1]. Furthermore, it is also confirmed that at low frequency, where the likelihood approach used here should coincide with the unbinned likelihood of [1], an 8% amplitude modulation would be discovered 50% of the times at the confidence level of 99%.

The comparison of the two methods described here and of the two adopted in [1] demonstrates that at low frequency the intrinsic statistical power of the methods is essentially the same. The superiority of the unbinned maximum likelihood used by the SNO Collaboration is in that it deals automatically better with the frequency, thus assuring a constant behaviour of the detection sensitivity as function of the frequency itself.

6. Specific frequencies

Annual modulation

It may be interesting to check how the annual modulation due to the Earth's orbit eccentricity is recovered from the data through the previous methodology. We consider for this case the results of the likelihood method for the combined dataset: the amplitude is evaluated to be 0.0337 ± 0.029 and the phase 0 ± 1.103 . In Fig. 16 the modulation described by the fitted amplitude and phase values is compared to that geometrically expected; the amplitude is picked up well by the fit, even though with a large error. For what concern the phase, there is a shift between the best fit and the expected curve of about 40 days.

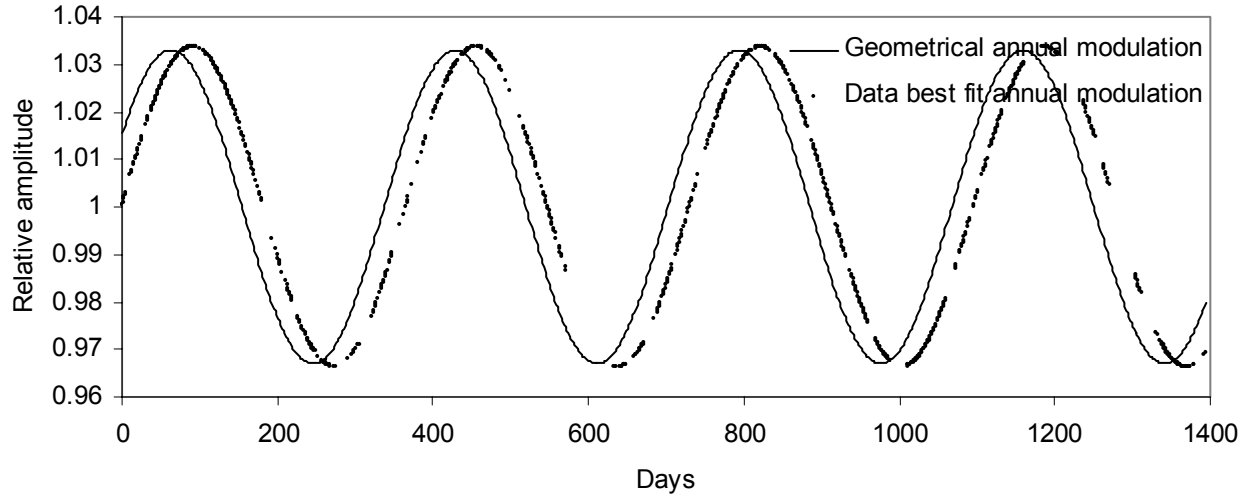


Figure 16 – Annual modulation

The spectral amplitude at this frequency is 2.26 and thus clearly well below the discovery capability of both methods. This fact is very clearly shown in Fig 17, where the expected spectral distribution of the annual modulation line of 3.3% relative amplitude is reported together with the global and single frequency noise distributions. The global noise distribution, in particular, masks completely the expected signal distribution, thus virtually preventing any detection possibility in a “blind” search over the entire investigated frequency range. The situation is better if one considers only the frequency of interest; but even in this case, by determining the detection threshold that would ensure on the exponential noise distribution a false alarm probability of 1%, it would give a detection probability of only about 14%. So, in other words, without knowing that such a modulation must be there, it could not be recognized. This is clearly not surprising, since the modulation amplitude is pretty low if compared with the Poisson scattering of the data.

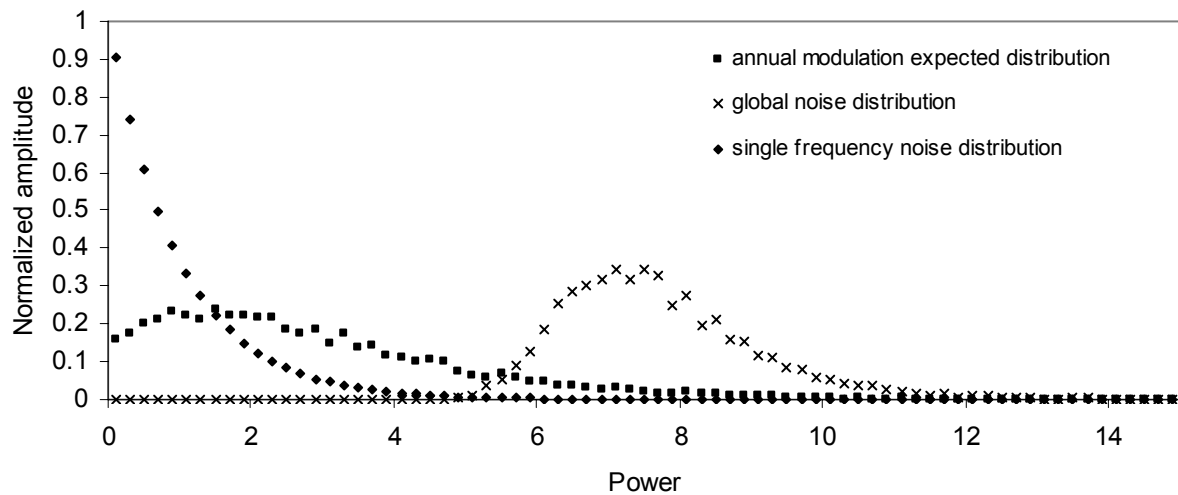


Figure 17 – Annual modulation: expected amplitude distribution

9.42 frequency

Recent analyses of the Super-Kamiokande I data [8][14] pointed toward a spectral feature at 9.42-9.43 cycles/year, with controversial significance, that, if interpreted as a true signal, would correspond to a modulation of relative amplitude between 6 and 7%. It is thus interesting to analyze in this respect the SNO data.

In Fig. 18 it is shown the expected amplitude distribution of the corresponding spectral ordinate assuming a true amplitude of 6.5 %, compared with the single frequency and global noise distributions. The broad signal distribution is largely masked by the noise distribution. Thus, also in such a case the “blind” search would hardly lead to discover the signal if present, but assuming the a-priori knowledge of the frequency to be searched the detection efficiency would be quite high; indeed fixing as above the 99% confidence level threshold on the exponential single frequency noise distribution, the corresponding detection probability would result equal to about 82.6%.

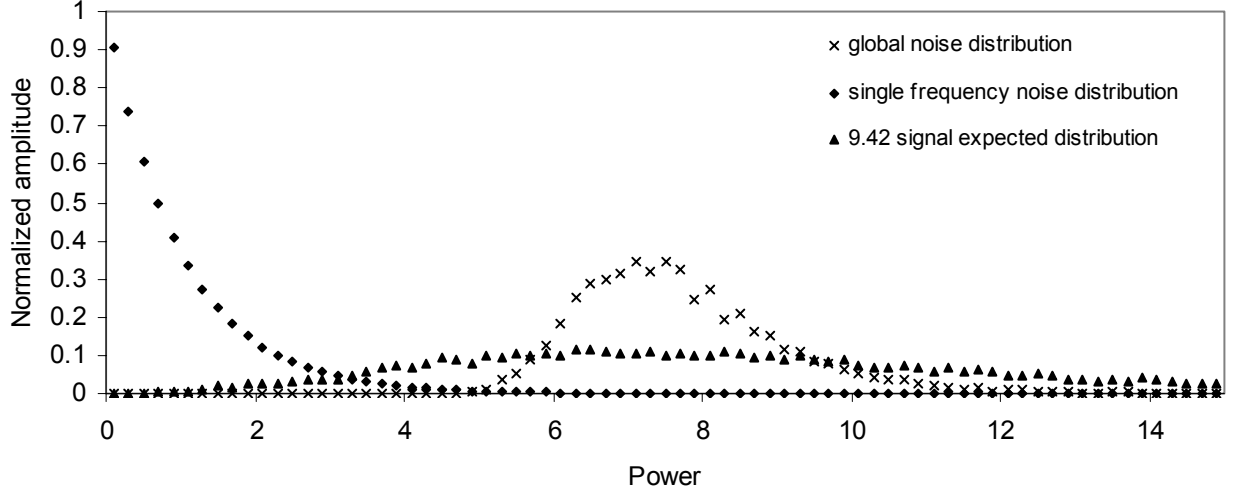


Fig. 18 – 9.42 cycles/year signal: expected amplitude distribution

In the combined likelihood spectrum in Fig.8, in the region between 9.32-9.52 cycles/year the maximum ordinate is 0.407 at the frequency of 9.41 (the corresponding amplitude best fit value is $0.0128^{+0.0228}_{-0.0128}$) This spectral value appears immediately inconsistent with the expected signal distribution in Fig. 18, since it lies on its extreme left tail region. Quantitatively, the Monte Carlo result gives a probability to get a value as low or lower of 0.407, given a signal actually present, less than 0.1 percent.

In summary, the SNO data are thus strongly in disagreement with the presence of a 9.42-9.43 cycles/year modulation, in the 6-7% amplitude range, in the measured ^8B solar neutrino flux.

7. How to approximate the unbinned likelihood approach

This digression which concludes the paper is intended to illustrate a methodology which exploits the released 1 day truncated data in a way suited to approximate the unbinned likelihood approach adopted by the SNO Collaboration. Essentially what it is proposed here is to write down a sort of “1 day binned” likelihood which takes into account the data taking period of each 1 day bin as it is, without thus resorting to the concept of weighted mean time adopted in the methods extensively developed in the previous paragraphs.

To this purpose, the actual number of counts measured in each bin is supposed drawn from a Poisson distribution with parameter μ_r given by

$$\mu_r = \sum_{r_k=1}^R \int_{t_{srk}}^{t_{erk}} \mu_{\cos t} [1 + a \cdot \sin(\omega t + \phi)] dt \quad (13)$$

where R is the number of data taking intervals in the r_{th} 1 day bin and t_{srk} and t_{erk} are the corresponding start and end times.

Following the notation used in paragraph 3.2, the “1 day binned” likelihood spectrum hence becomes

$$S(\omega) = \max_{a,\varphi} \sum_{r=1}^N (-\mu_r + n_r \cdot \ln \mu_r) - \sum_{r=1}^N (-\mu_{\cos t} + n_r \cdot \ln \mu_{\cos t}) \quad (14)$$

that, because of the Wilks’ theorem, is exponentially distributed as e^{-S} under the null hypothesis.

Due to the intensive computing requirements of such a methodology, in the following only the case of the combined dataset will be considered, whose spectrum according eq. (14) is shown in Fig. 19.

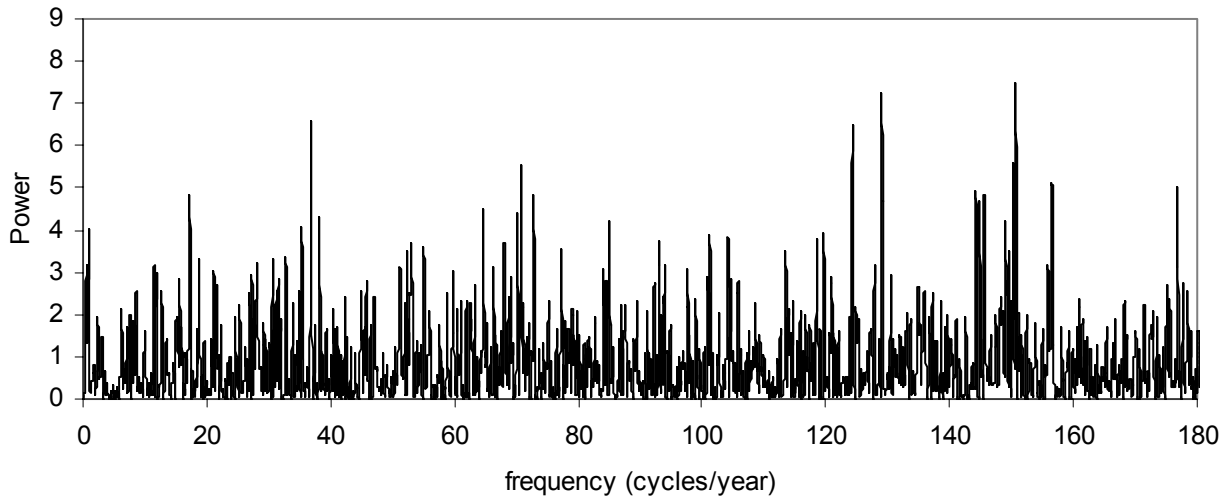


Fig.19 – Combined dataset 1 day binned likelihood spectrum

In the spectrum the four highest peaks have, respectively, ordinates 7.46 (150.69), 7.23 (129.05), 6.60 (36.84) and 6.51 (124.31) (again in parenthesis there are the corresponding frequencies in cycles/year).

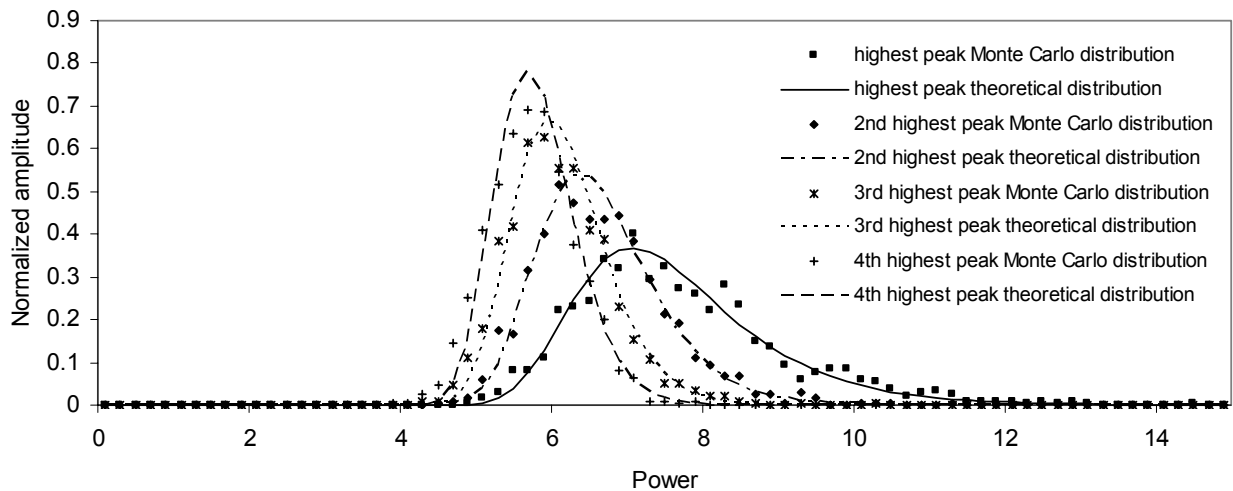


Fig. 20 – Combined dataset null hypothesis distributions (1 day binned likelihood method)

The corresponding null hypothesis distributions, evaluated through a set limited to 1000 simulations because of the computing constraints mentioned above, are reported in Fig. 20. Also in this case the peak distributions follow only approximately the model functions, far from the good

agreement observed in the Lomb-Scargle case, with an M value obtained through the approximate fit of the highest peak distribution to the equation (5) equals to 1182. From such distributions it can be inferred that the significance of the highest peak is 49.7%, of the second highest is 22.1%, of the third highest 22.0%, and finally of the fourth highest 9.7%. Therefore, also such methodology produces a spectrum perfectly consistent with the constant rate hypothesis, further confirming the results obtained with the previous analyses.

Finally, in Fig. 21 the sensitivity plot of Fig. 15 is updated with the addition of the sensitivity contours stemming from this more refined methodology; as expected at low frequency the sensitivity of the 50% and 90% contours reproduce that relevant to the approximate likelihood method, while at high frequency the new contours show an enhanced discovery capability, due to the more precise account of the actual run times within each nominal 1 day bin.

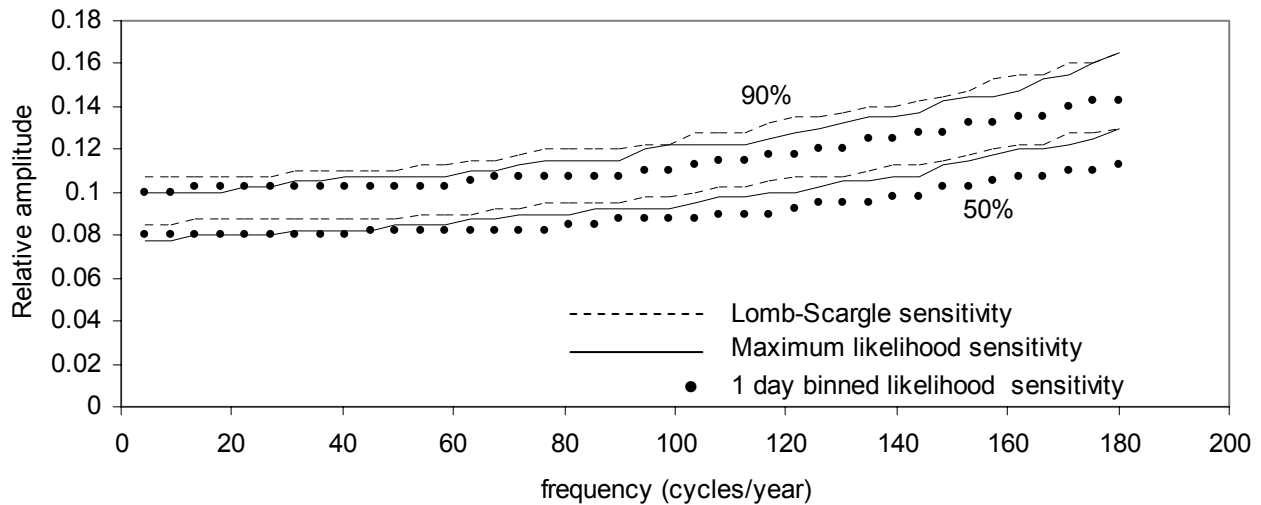


Figure 21 – Sensitivity contours

8. Conclusions

The data released by the SNO collaboration related to the D_2O and salt phases of the experiment have been searched for time modulations through the standard Lomb-Scargle method and a likelihood extension of the Lomb-Scargle method itself. Both methodologies, applied either on each dataset or on the combined dataset did not reveal any hint of periodicities, within the sensitivity limits dictated by the noise (Poisson scattering) affecting the data series. The sensitivity to true oscillations has been evaluated, as well, leading to a discovery probability (in case of the likelihood method) of 50% for a low frequency oscillation with relative amplitude of 8% at the confidence level of 99%. The data have been specifically examined for the periodicity of 9.42-9.43 cycles/year stemming from some analysis of the Super-Kamiokande I data, showing that the SNO results are strongly disfavoured an oscillation at that frequency in the 6-7% amplitude range in the 8B solar neutrino flux.

Aknowledgements

The authors would like to thank the SNO Collaboration for making the data publicly available. G. Ranucci acknowledges also the very fruitful exchange of communications with Scott Oser.

References

- [1] B. Aharmim et al. "Search for periodicities in the 8B solar neutrino flux measured by the Sudbury Neutrino Observatory SNO", Physical Review D, vol. 72, Issue 5, September 2005, id. 052010
- [2] <http://sno.phy.queensu.ca/sno/periodicity/>

- [3] Horne, J, H..and Baliunas, S., L., "A prescription for period analysis of unevenly sampled time series", *Astrophysical Journal*, vol. 302, March 15, 1986, p. 757-763
- [4] J.D. Scargle, "Studies in astronomical time series analysis. III – Fourier Transforms, autocorrelation functions, and cross-correlation functions of unevenly spaced data ", *Astrophysical Journal*, vol. 343, Aug. 15, 1989, p. 874-887
- [5] J.Yoo et al., "Search for periodic modulations of the solar neutrino flux in Super-Kamiokande-I", *Physical Review D*, vol. 68, Issue 9, November 2003, id. 092002
- [6] N.R. Lomb, "Least-squares frequency analysis of unequally spaced data", *Astrophysics and Space Science*, vol. 39, Feb. 1976, p. 447-462
- [7] J.D. Scargle, "Studies in astronomical time series analysis. II - Statistical aspects of spectral analysis of unevenly spaced data", *Astrophysical Journal*, Part 1, vol. 263, Dec. 15, 1982, p. 835-853
- [8] G. Ranucci, "Likelihood scan of the Super-Kamiokande I time series data", *Physical Review D*, vol. 73, Issue 10, May 2006, id. 103003
- [9] W.H. Press et al., "Numerical recipes in Fortran ", Cambridge University Press (1991), sect. 12.1 and sect. 13.8
- [10] G. Ranucci, "Time statistics of the photoelectron emission process in scintillation counters", *Nucl. Instr. and Meth. A*335, 15 October 1993, p. 121-128
- [11] Wang Zhaomin et al, "The influence of average photon number on the measured fluorescence decay time of scintillator ", *Nucl. Instr. and Meth. A*419, 11 December 1998, p. 154-159
- [12] P.A. Sturrock et al., "Search for Periodicities in the Homestake Solar Neutrino Data", *Astrophysical Journal* v.491, December 1997, p.409
- [13] S.S. Wilks, "The large-sample distribution of the likelihood ration for testing composite hypotheses ", *Ann. Math. Stat.*, 9, (1938) 60-62
- [14] P.A. Sturrock et al., "Power-spectrum analyses of Super-Kamiokande solar neutrino data: Variability and its implications for solar physics and neutrino physics" *Physical Review D*, vol. 72, Issue 11, December 2005, id. 113004